JOURNAL OF NEUROTRAUMA 30:546–556 (April 1, 2013)

DOI: 10.1089/neu.2012.2416

Monitoring Functional Impairment and Recovery after Traumatic Brain Injury in Rats by fMRI

Juha-Pekka Niskanen,[1,2] Antti M. Airaksinen,[1] Alejandra Sierra,[1] Joanna K. Huttunen,[1] Jari Nissinen,[3] Pasi A. Karjalainen,[2] Asla Pitkänen,[3,4] and Olli H. Gröhn[1]

Abstract

The present study was designed to test a hypothesis that functional magnetic resonance imaging (fMRI) can be used to monitor functional impairment and recovery after moderate experimental traumatic brain injury (TBI). Moderate TBI was induced by lateral fluid percussion injury in adult rats. The severity of brain damage and functional recovery in the primary somatosensory cortex (S1) was monitored for up to 56 days using fMRI, cerebral blood flow (CBF) by arterial spin labeling, local field potential measurements (LFP), behavioral assessment, and histology. All the rats had reduced blood-oxygen-level-dependent (BOLD) responses during the 1st week after trauma in the ipsilateral S1. Forty percent of these animals showed recovery of the BOLD response during the 56 day follow-up. Unexpectedly, no association was found between the recovery in BOLD response and the volume of the cortical lesion or thalamic neurodegeneration. Instead, the functional recovery occurred in rats with preserved myelinated fibers in layer VI of S1. This is, to our knowledge, the first study demonstrating that fMRI can be used to monitor post-TBI functional impairment and consequent spontaneous recovery. Moreover, the BOLD response was associated with the density of myelinated fibers in the S1, rather than with neurodegeneration. The present findings encourage exploration of the usefulness of fMRI as a noninvasive prognostic biomarker for human post-TBI outcomes and therapy responses.

Key words: electrophysiology; MRI; recovery; sensory function; TBI

Introduction

Traumatic brain injury (TBI) is a major cause of death and disability worldwide, with an estimated 10,000,000 affected annually.[1] After the initial damage caused by the direct mechanical force to the head, secondary damage develops over a period of time extending from hours to months.[2] It consists of a myriad of molecular changes that underlie the reorganization of cellular networks, including neurodegeneration, axonal injury, axonal plasticity, neurogenesis, glial activation, angiogenesis, blood–brain barrier damage, and invasion of peripheral inflammatory cells.[2–5]

The molecular and cellular reorganization patterns that follow TBI are accompanied by hemodynamic alterations.[6–10] Depending upon severity, TBI can lead to long-lasting disabilities, such as motor and cognitive impairment, psychiatric comorbidities, and post-traumatic epilepsy.[3,11,12]

The therapeutic window for recovery-enhancing treatments and antiepileptogenesis includes the time period of secondary damage and consequent repair. Therefore, noninvasive methods designed to provide *in vivo* monitoring of the post-injury aftermath of pathology and its repair, as well as any functional recovery, would provide tools to predict disease outcomes as well the efficacies of possible treatments.

The spectrum of secondary damage and associated functional impairment are, however, difficult to assess using structural imaging alone. This relates to recent observations that demonstrate how neuronal networks that appear structurally undamaged can still contribute to functional impairment because of their aberrant intracellular or intercellular signaling.[13,14] Several neuroimaging methods have been applied to study brain function in patients with TBI, including positron emission tomography (PET),[15] cerebral blood flow (CBF),[9] cerebral blood volume (CBV),[16] and functional magnetic resonance imaging (fMRI).[17–19] The major limitation in patient studies relates to the lack of histological verification of imaging findings. Even though several clinically relevant animal models of TBI are available,[20] studies applying functional imaging after experimental TBI are scarce. A few studies have focused on post-TBI changes in CBF and CBV.[8,21,22] So far, only Henninger and colleagues[23] have investigated blood-oxygen-level-dependent (BOLD) responses and fMRI activation patterns after TBI, using a weight-drop model with mild severity.

[1]Department of Neurobiology and [3]Department of Neurobiology, Epilepsy Research Laboratory, A. I. Virtanen Institute for Molecular Sciences, and [2]Department of Applied Physics, University of Eastern Finland, Kuopio, Finland.
[4]Department of Neurology, Kuopio University Hospital, Kuopio, Finland.

We hypothesize that functional impairment and favorable functional recovery could be monitored after moderate experimental TBI in rats by observing the post-TBI BOLD response. We tested this hypothesis by investigating the recovery of the BOLD fMRI response in the rat somatosensory cortex (S1) over a follow-up period of 56 days after lateral fluid percussion induced brain injury (FPI) in rats. The S1 cortex was chosen for analysis, as its BOLD response to electrical forepaw stimulation is both reliable and highly reproducible in rats. Furthermore, in our pilot experiments as well as in a previous study with a rat weight-drop model,[23] S1 showed remarkable post-TBI suppression of the BOLD response even though no changes were seen on T_2-weighted MRI, suggesting that many of the neuronal elements required for favorable plasticity are still present. We also measured the local field potentials (LFP) in S1, determined the CBF with arterial spin labeling (ASL), and, finally, we investigated the severity of neurodegeneration and damage of myelinated axons along the somatosensory thalamocortical pathway histologically.

Methods

The study design is shown in Figure 1.

Animals

Adult male Sprague–Dawley rats weighing 293–322 g at the time of TBI were used ($n = 26$, Harlan Netherlands B.V., Horst, the Netherlands). After injury, animals were housed in individual cages and kept under a normal 12 h light/12 h dark cycle (lights on at 07:00 a.m.), constant temperature (22 ± 1°C), and humidity (50–60%). Water and food were available *ad libitum.* All animal procedures were approved by the Animal Ethics Committee of the Provincial Government of Southern Finland, and conducted in accordance with the guidelines of the European Community Council Directives 86/609/EEC.

Lateral FPI

TBI was induced by lateral FPI as previously described.[24,25] Of 26 rats, 18 were injured and 8 were sham operated. Briefly, animals were anesthetized with a mixture containing sodium pentobarbital (58 mg/kg), chloral hydrate (60 mg/kg), magnesium sulfate (127.2 mg/kg), propylene glycol (42.8%), and absolute ethanol (11.6%), (i.p., 6 mL/kg). A 5 mm diameter craniectomy was performed over the left parietal cortex, leaving the dura intact. The center of the craniectomy was located halfway between bregma and lambda, with the lateral edge of the craniectomy adjacent to the left lateral ridge. A rigid plastic cap cut from a female Luer-Lok needle hub was inserted into the hole over the intact dura, sealed to the skull with Vetbond glue, and filled with 0.9% NaCl to check the quality of the seal and to prevent the dura from drying out. The injury cap was then cemented onto the skull with dental acrylic. A 90 min interval separated the induction of anesthesia and the injury. TBI was produced by a fluid percussion device (AmScien Instruments, Richmond, VA). A brief (21–23 ms) transient pressure fluid pulse impact was applied against the exposed dura. Pressure pulses were measured extracranially by a transducer and recorded on a storage oscilloscope. The pressure of the impact was adjusted to induce a moderate TBI (≈ 2 atm, mortality within the first 48 h $< 20\%$).

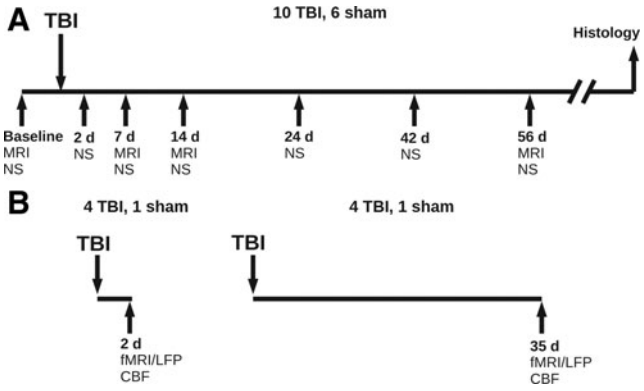

FIG. 1. Study design. **(A)** Group A (10 rats with traumatic brain injury [TBI], 6 sham operated rats) was imaged at baseline, and thereafter at 7 days, 14 days, and 56 days post-TBI. Motor recovery was monitored by behavioral assessment of composite neuroscore at baseline and during the following 56 days. Finally, rats were perfused for histology 84 days after TBI. **(B)** Group B (8 TBI, 2 sham operated) was subdivided into two groups, each consisting of four TBI and one sham-operated animals, to be imaged either at 2 days or 35 days post-TBI by using cerebral blood flow (CBF) as well as simultaneous functional MRI and local field potential (LFP) measurements.

The animals were further divided into two experimental groups (Fig. 1). In group A ($n = 16$, 10 with TBI and 6 with sham operation), rats were investigated at multiple time points using MRI, behavioral assessment, and end-point histology to reveal the dynamics of functional and structural changes in S1. In Group B ($n = 10$, 8 TBI and 2 sham-operated), each animal was measured only at one time point, either 2 days (4 TBI, 1 sham) or 35 days (4 TBI, 1 sham) after surgery, to assess post-TBI functional changes in blood perfusion and electrophysiology in the S1 by measuring CBF using ASL as well as fMRI combined with simultaneous measurements of somatosensory LFPs.

Anesthesia and animal preparation for MRI

Rats were first anesthetized with isoflurane (4% for induction and 1.5% for maintenance) in an N_2/O_2 (70%/30%) mixture and fixed into an in-house made nonmagnetic stereotactic frame with a bite bar and earplugs. A pair of small needles (27 G) was inserted into both forepaws for electrical stimulation. A subcutaneous infusion line (PE-10, Intramedic™ Clay Adams Brand, Polyethylene Tubing) was inserted at the neck to administer medetomidine. Then the rat was placed into the MRI scanner, and isoflurane anesthesia was switched to medetomidine sedation (0.02 mg/kg bolus of medetomidine followed by 0.1 mg/kg/h infusion starting 10 min later; DOMITOR®, Orion Pharma, Espoo, Finland). Animals were allowed to spontaneously inhale a mixture of 70% N_2–30% O_2, and their respiration rate was monitored throughout the experiment (MR-Compatible, Model 1025 Monitoring & Gating system, SA Instruments, Inc., USA). The temperature of the holder was maintained constant by circulating warm water (37.0 ± 0.5°C) through a heating pad (HETO, Denmark, Heating Shaking Waterbath). To reverse the medetomidine sedation after MRI in group A, rats were administered 0.1 mg/kg of atipamezole hydrochloride dissolved in 0.9% NaCl (i.p., 2 mL/kg, ANTISEDAN®, Orion Pharma, Espoo, Finland) and 2.0 mL of saline-glucose (50 mg/mL) solution. To monitor blood gases and pH at the onset of MRI in group B, the femoral artery was cannulated, blood samples were taken via an arterial catheter (volume 0.15 mL), and immediately analyzed using an i-STAT portable clinical analyzer (Abbott Laboratories Inc.).

Electrophysiology

Implantation of electrodes for LFP recordings. LFPs were recorded in the ipsilateral and contralateral somatosensory cortex simultaneously with fMRI from animals in group B. To insert the LFP electrodes, the scalp was removed and a small hole was drilled in the skull over the left (just rostral to the craniectomy) and right somatosensory cortices (AP -0.5 to -1.0 mm, ML 4 mm from

bregma, according to Paxinos and Watson[26]). The dura was incised and MRI-compatible insulated electrodes made from tungsten wire (diameter 50 μm, California Fine Wire, Grover Beach, CA) were inserted into the S1 at a depth of 0.5–1.0 mm from the surface of the brain using a stereotactic electrode holder. The electrodes were bent toward the neck and glued to the skull (Super Glue, Bison International, Goes, The Netherlands). Gelfoam gelatin sponge (Pfizer, New York, NY) was used to fill the hole in the skull to prevent the glue from irritating the brain. Chloridized silver wire (Ag/AgCl) reference and ground electrodes were placed subcutaneously at the rat's neck.

Forepaw stimulation. Left and right forepaws were separately stimulated using bipolar square wave pulses (9 Hz, 0.3 ms, 2.0 mA; A-M Systems, Sequim, WA).

Analysis of LFP signal. Spontaneous and evoked LFP signals were recorded using a BrainAmp MR plus MRI compatible biosignal amplifier (Brain Products GmbH, Munich, Germany, sampling rate 5 kHz, low-pass filter 1 kHz cutoff) and analyzed with in-house made Matlab code. First, the stimulation events were detected using stimulus markers embedded in the LFP data files during the recording. The amplitudes of the responses were estimated by subtracting a baseline value (average amplitude calculated from a 6 ms window before the stimulation event) from the minimum amplitude of the signal in a fixed window of 40 ms (200 data points, covering the entire duration of the evoked response). The response latencies were calculated as the time period from the stimulation event to the signal minimum in the fixed time window. Responses that were contaminated with MRI artifacts were rejected from the analysis.

MRI

All MRI experiments were performed using a 4.7 T horizontal scanner (Magnex Scientific Ltd., Oxfordshire, UK) interfaced with a Varian UNITYInova console (Varian Inc., Palo Alto, CA). An actively decoupled volume radiofrequency coil and quadrature surface coil pair (RAPID Biomedical GmbH, Rimpar, Germany) were used for signal transmission and reception. In group A, imaging was performed at baseline and at 7, 14, and 56 days after TBI or sham operation. In group B, 50% of the animals (4 TBI, 1 sham) were randomized to be imaged at 2 days, and the other 50% at 35 days post-TBI. One injured rat from the 2 day group was not imaged because of technical difficulties.

After switching from isoflurane anesthesia to medetomidine sedation, the rat's condition was allowed to stabilize for $\sim$30 min. This time period was used for RF pulse calibration, shimming and acquiring structural T_2-weighted MR images (multislice spin-echo, TR = 2.5 sec, TE = 60 ms, 256 × 256 matrix, field of view [FOV] = 5 cm × 5 cm, slice thickness 1.5 mm, voxel size 0.195 × 0.195 × 1.5 mm, 14 slices). For group A, the functional imaging slice was positioned axially to the somatosensory cortex at 1 mm posterior from bregma as guided by the horizontal pilot scans. For group B, the functional imaging slice was positioned 1.1 mm posterior from bregma (0.5 mm caudal from the electrode) to minimize the susceptibility artifacts caused by the electrode that was used for simultaneous LFP recordings. After local shimming with FASTMAP,[27] the proton line width at half of maximum was between 10 and 15 Hz in the imaging slice. Functional MR data were acquired using a single-shot spin-echo echo-planar imaging sequence (TR 2 sec, TE 60 ms, slice thickness 1.5 mm, FOV 2.5 cm × 2.5 cm, 64 × 64 matrix, voxel size $0.39 \times 0.39 \times 1.5\,mm^3$) during electric stimulation (bipolar pulses, 9 Hz, 0.3 ms, 2.0 mA) of the right and left forepaws separately in a randomized order. The stimulus paradigm consisted of seven phases: baseline (30 images) – activation (15 images) – baseline – activation – baseline – activation – baseline. Four dummy scans and a reference scan were acquired before collecting functional data. The total number of functional images was 165 corresponding to a total imaging time of 5 min and 40 sec for a single forepaw stimulation.

Measurement of CBF was performed for the animals in group B. CBF was quantified using continuous ASL[28] with a fast spin echo (FSE) read out (TR = 3 sec, TE_{eff} = 7 ms, FOV = 4 × 4 cm, 128 × 128 matrix, echo train length [ETL] = 16, slice thickness 2 mm, voxel size $0.31 \times 0.31 \times 2.0\,mm^3$). Subtraction images from six pairs of label and control images were used to calculate the CBF map of the functional slice. Inversion recovery FSE with an adiabatic inversion pulse (TR = 5 sc, TE_{eff} = 7 ms, FOV = 4 × 4 cm, 128 × 128 matrix, voxel size $0.31 \times 0.31 \times 2.0\,mm^3$, ETL = 16, TI = [5, 300, 600, 1000, 1500] ms) was used to obtain T_1 maps to be used in calculation of absolute CBF values.

Composite neuroscore

Assessment of motor function by neuroscore has been used as a standard measure of injury severity in the lateral FPI model.[29] Here we used post-injury neuroscore as an indicator that the injury severity produced in the experimental group was comparable to moderate injury. We were also interested in monitoring whether there was any association in the recovery of motor and somatosensory modalities. Motor recovery of rats in group A was assessed using composite neuroscore at baseline and at 2, 7, 14, 28, 42, and 56 days post-TBI.[24,25] Briefly, animals were given a score from 0 (severely impaired) to 4 (normal) for each of the following seven indices: (i-ii) left and right (two indices) forelimb flexion during suspension of the tail, (iii-iv) left and right (two indices) hindlimb flexion when the forelimbs remain on the hard surfaces and the hindlimbs are lifted up and back by the tail, (v-vi) ability to resist a lateral propulsion toward the left and right (two indices), and (vii) angle board. A composite neuroscore (0–28 points) was generated by combining the scores for each of these seven tests. To assess the speed of recovery, we calculated the recovery rate for each animal as a slope of the line drawn between the neuroscores of 2 days and 14 days.

Histology

Fixation and tissue processing. After imaging (i.e., 87–113 days post-TBI), the brains of rats in group A were processed for histology. Briefly, the rat was deeply anesthetized and perfused transcardially with 0.9% NaCl for 2 min followed by 4% paraformaldehyde in 0.1 M sodium phosphate buffer (PB, pH 7.4) for 20 min. The brain was removed from the skull and postfixed in the same fixative for 4 h at 4°C. It was then placed in a cryoprotectant (20% glycerol in 0.02 M potassium phosphate buffered saline (KPBS, pH 7.4) for 36 h. Thereafter, it was blocked, frozen on dry ice, and stored at −70°C until cut. The brains were sectioned in the coronal plane (30 μm of thickness, 1-in-5 series) with a sliding microtome. The first series of sections was stored in 10% formalin at room temperature and the remaining series in tissue-collecting solution (TCS) (30% ethylene glycol and 25% glycerol in 0.05 M PB) at −20°C until processed.

Nissl staining and assessment of neurodegeneration. The first series of sections was stained for thionin to identify the cytoarchitectonic boundaries as well as distribution and severity of neuronal damage in the cortex and thalamus. The severity of neurodegeneration in the ventral posterior complex of the thalamus was scored as follows: score 0, no neuronal loss; score 1, <20%; score 2, 20–50%; score 3, >50% neuronal loss according to Pitkanen et al.[30]

Assessment of density of myelinated fibers in S1. After locating the level of S1 in thionin-stained sections that corresponded to the fMRI slice, three adjacent coronal sections (150 μm apart) were collected from TCS, washed three times in 0.02 M

KPBS (10 min each), mounted on gelatin-coated slides, and dried at 37°C overnight. Sections were incubated in 0.2% gold chloride solution ($HAuCl_4$·3H2O, G-4022 Sigma) made in 0.02 M PB (pH 7.4) containing 0.09% NaCl in the darkroom for 11–14 h (at room temperature). The slides were then washed in 0.02 M PB twice (4 min each), and placed in 2.5% sodium thiosulfate solution for 5 min. After 3×10 min washes in 0.02 M PB containing 0.09% NaCl, sections were dehydrated through an ascending series of ethanol, cleared in xylene, and cover-slipped with DePeX (BDH, Laboratory Supplies, Dorset, UK).

The density of myelinated fibers in the somatosensory cortex (S1) was quantified using ImageJ software (version 1.41o, http://rsb.info.nih.gov/ij). Briefly, digital images were captured from each section using a Leica DMRB microscope equipped with a Nikon DXM1200F digital camera. After conversion of the images to gray scale, optical density was obtained from three circular regions of interest (ROI, diameter 78 μm) in layer VI of S1 both ipsilaterally and contralaterally. Background staining was calculated from three ROIs (diameter 78 μm) placed in layer I (myelin free) of the same section of S1 both ipsilaterally and contralaterally. Finally, the density of labeling in layer VI of S1 for each rat was calculated as (mean intensity of background ROIs – mean intensity of labeling in ROIs)/intensity of background ROIs.

Analysis of MRI data

Volume of the lesion in the cortex (V_{Cx}) at different time points in group A was analyzed using Aedes 1.0 (http://aedes.uku.fi). Briefly, the region showing hyperintensity in T_2-weighted multislice images was outlined in three consecutive slices (1.5 mm each) encompassing the entire lesion area.

We also calculated the ratio of the ipsilateral and contralateral cortical volumes (R_{Cx}). For this analysis, the volume of the ipsilateral cortex was obtained by first outlining the entire ipsilateral cortex, and then subtracting the lesion volume from it. Next, the R_{Cx} was calculated by dividing the ipsilateral cortical volume by the contralateral cortical volume.

The CBF maps for group B were estimated from the ASL MRI data by calculating the difference between the control and label images, and using T_1 relaxivity maps and a λ value of 0.9 $mL \cdot g^{-1}$ to calculate absolute perfusion values.[28] The average perfusion values were calculated from the 2×2 voxel ROIs that were drawn on both the ipsilateral and contralateral S1.

The fMRI activation patterns were calculated using SPM5 (Wellcome Department of Imaging Neuroscience, University College London, UK) along with in-house made code written in Matlab R2007b (MathWorks, Natick, MA). Preprocessing of the fMRI data included motion correction and spatial smoothing with a 2×2 voxel full width at half maximum Gaussian kernel. A Gaussian hemodynamic response function (HRF) was used instead of the SPM5 default canonical HRF. The parameters of the Gaussian HRF were selected to reflect the temporal characteristics of the measured rodent HRF reported by Silva and colleagues,[31] resulting in an HRF peaking at 2 sec and returning back to baseline at 5 sec.

The statistical analyses of fMRI data were performed using the general linear model on a voxel-by-voxel basis. A block design model based on the forepaw stimulation paradigm was used as a regressor (30 baseline points followed by 15 activation points repeated three times with a 30 point baseline period at the end). A temporal high-pass filter with a 256 second cutoff was applied for filtering low frequency signal drifts. The brain areas activated in response to forepaw stimulation were assessed using a one-sample t test thresholded at $p \leq 0.05$ (false discovery rate [FDR] corrected).

ROI analysis was performed on the fMRI time series to obtain group statistics of the somatosensory BOLD responses and to assess the strength of the BOLD response in S1. The average time series were extracted from 2×2 voxel ROIs drawn on the primary somatosensory cortices ipsi- and contralaterally to the FPI site. The corresponding anatomical images and the Paxinos rat brain atlas[26] were consulted as a reference. The strength of the BOLD response was estimated by fitting the stimulus paradigm convolved with the HRF to the somatosensory time series after removing the linear trend.

The rate of the recovery of the BOLD response was estimated for animals in group A as a slope of the line drawn between ipsilateral BOLD responses at 7 days, 14 days, and 56 days after TBI.

Finally, we assessed the recovery index from the BOLD response of individual animals to classify them into recoverers and nonrecoverers. We defined ''impairment'' as the difference between the BOLD responses at baseline and at 7 days post-TBI. ''Recovery'' was defined as the difference in BOLD response at 7 days and 56 days post-TBI. The recovery index was then calculated by dividing recovery with impairment. Rats with a recovery index > 0.5 were considered recoverers, and those with an index < 0.5 were regarded as nonrecoverers.

Statistical analysis

All statistical analyses were performed using the Statistics Toolbox in Matlab R2007b (Mathworks, Natick, MA). Friedman's test followed by post-hoc analysis with Wilcoxon's signed rank test were used to assess interhemispheric differences in BOLD responses in injured and sham operated animals. Wilcoxon's test was also used to analyze the interhemispheric differences in CBF and in histological parameters. The Mann–Whitney U test was used to compare findings between sham operated and injured animals. A p value < 0.05 was considered to be significant and Boferroni correction was used to adjust the null hypothesis rejection level for multiple comparisons when required. All data are presented as mean ± standard deviation (SD).

Results

Mortality

There was no mortality during the first 48 h post-TBI, which is in line with previous studies showing that an impact severity of 2.06 ± 0.09 atm used in the present study results in moderate TBI.[5]

MRI

Analysis of blood gases and pH. At the onset of MRI measurements, blood samples were taken from the animals in group B. The mean arterial blood pCO_2 for all animals (four TBI, two sham operated) was 55.1 ± 9.1 mm Hg, pO_2 120.9 ± 31.6 mm Hg, and pH 7.34 ± 0.05. Blood gases of two sham operated animals were within the SD of TBI animals. No blood samples were taken from animals in group A, as repeated cannulation of the femoral artery could have compromised the well-being of the animals, and consequently the data collection over the 56 day follow-up.

Cortical lesion volume and appearance of S1. At the primary injury site in the temporoparietal cortex, most of the animals showed a variable degree of hyperintensity in structural T_2-weighted MR images. The primary cortical lesion was associated with perilesional hemorrhage and/or ventricular enlargement (Fig. 2A–C). At 7 days post-TBI, when the BOLD fMRI follow-up began, the lesion volumes in different animals varied from 0 to 4.4 mm^3 and cortical hyperintensity decreased during the 56 day follow-up. At all time points and in all animals, the more rostrally located S1 showed no changes in T_2-weighted MR images (Fig. 2D). In some TBI animals there was slightly more ventricular enlargement compared with sham operated animals (Fig. 2E-H).

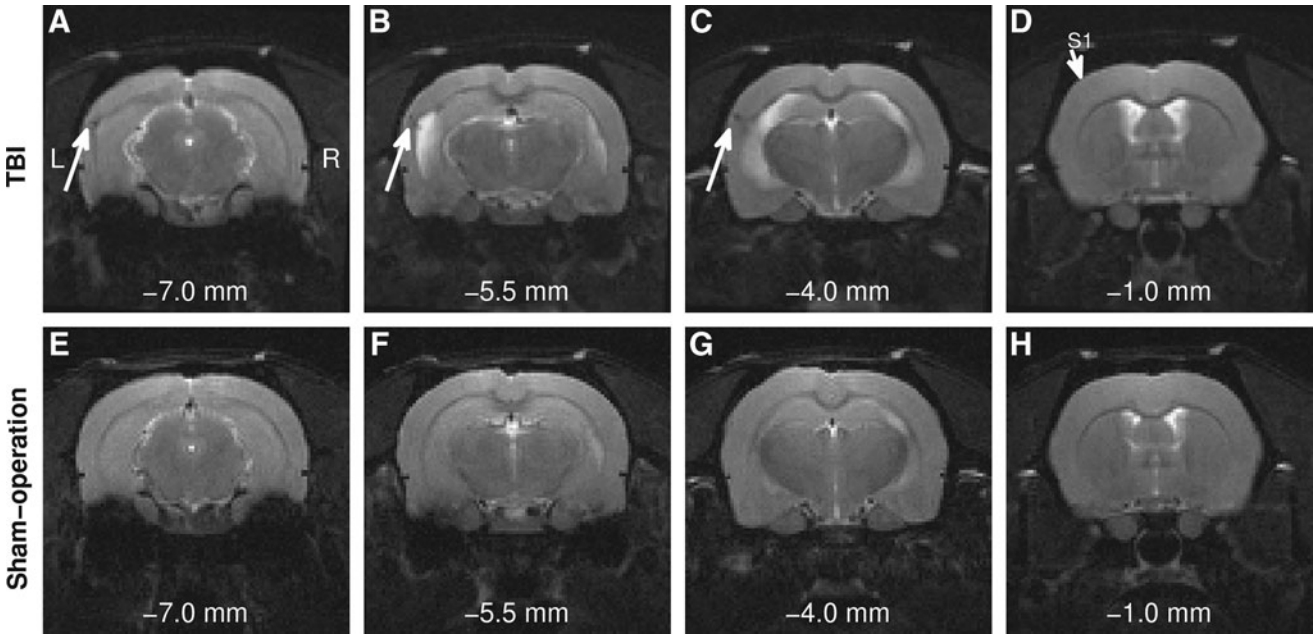

FIG. 2. T_2-weighted images of two representative rat brains at 56 days after traumatic brain injury (TBI) (upper row, **A–D**) and sham-operation (lower row, **E–H**). The arrow in panels **A–C** point to the lesion located caudal to the primary somatosensory cortex (S1, panel **D**) that showed no changes compared with S1 of the sham operated animals **(H)**. The numbers indicate the slice position relative to the bregma (**A** and **E** most caudal, **D** and **H** most rostral).

fMRI. Rats in group A were followed up with fMRI for 56 days post-TBI. At 7 days post-injury, the ipsilateral S1 fMRI activation was completely or partially lost in 8 of 10 rats with TBI and the strength of the BOLD response was reduced in all TBI animals ($p < 0.008$ compared with the baseline BOLD response of the same animals). The BOLD response showed a slow recovery between 7 and 56 days ($p < 0.03$). However, because of remarkable inter-animal variability in BOLD after TBI, the significance in the increase in BOLD response was lost after adjustments for multiple comparisons. Therefore, we next assessed the recovery in individual animals. We found that in 4 of 10 rats, the recovery index of the ipsilateral somatosensory BOLD response was ≥ 0.5 during the 56 day follow-up, suggesting a favorable recovery in a subpopulation of animals (Figs. 3 and 4A–C).

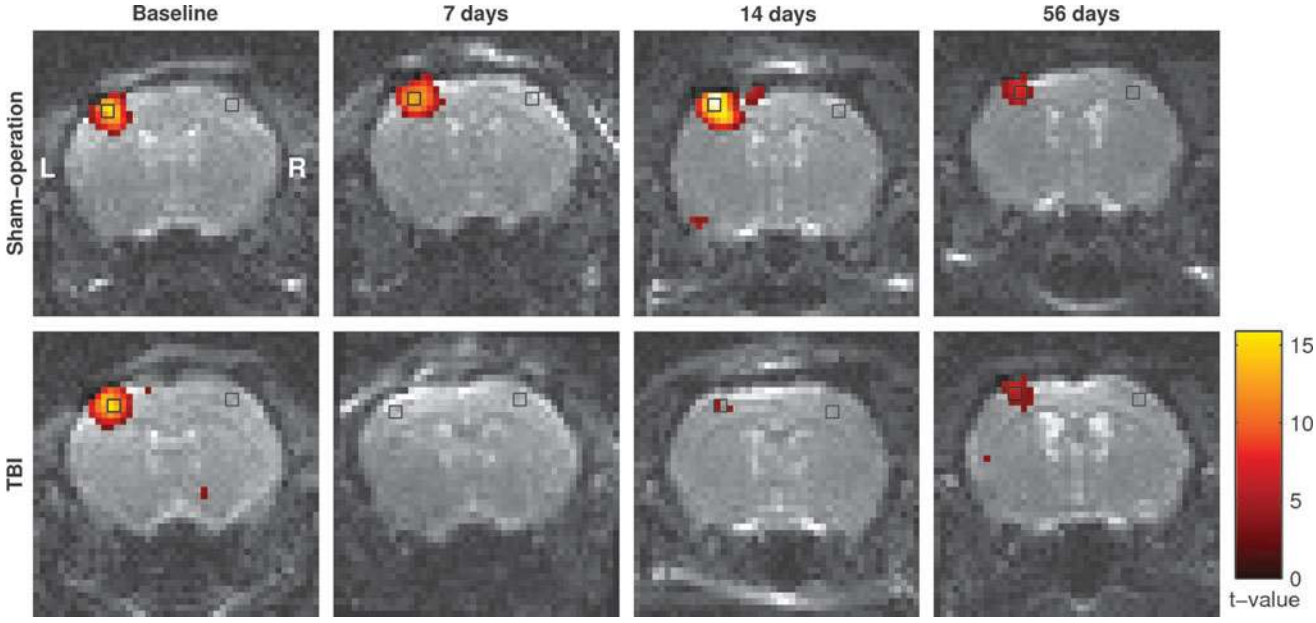

FIG. 3. Representative examples of functional MRI (fMRI) activation maps in a sham-operated animal (upper panels) and in a rat with traumatic brain injury (TBI) (lower panels) during the 56 day follow-up. Activation was triggered by electrical stimulation of the right forepaw before injury (or sham operation) and at 7, 14, and 56 days after TBI. fMRI activation maps are overlaid on EPI images. The regions of interest (ROIs) for extracting average fMRI time series are shown as black squares. Color image is available online at www.liebertpub.com/neu

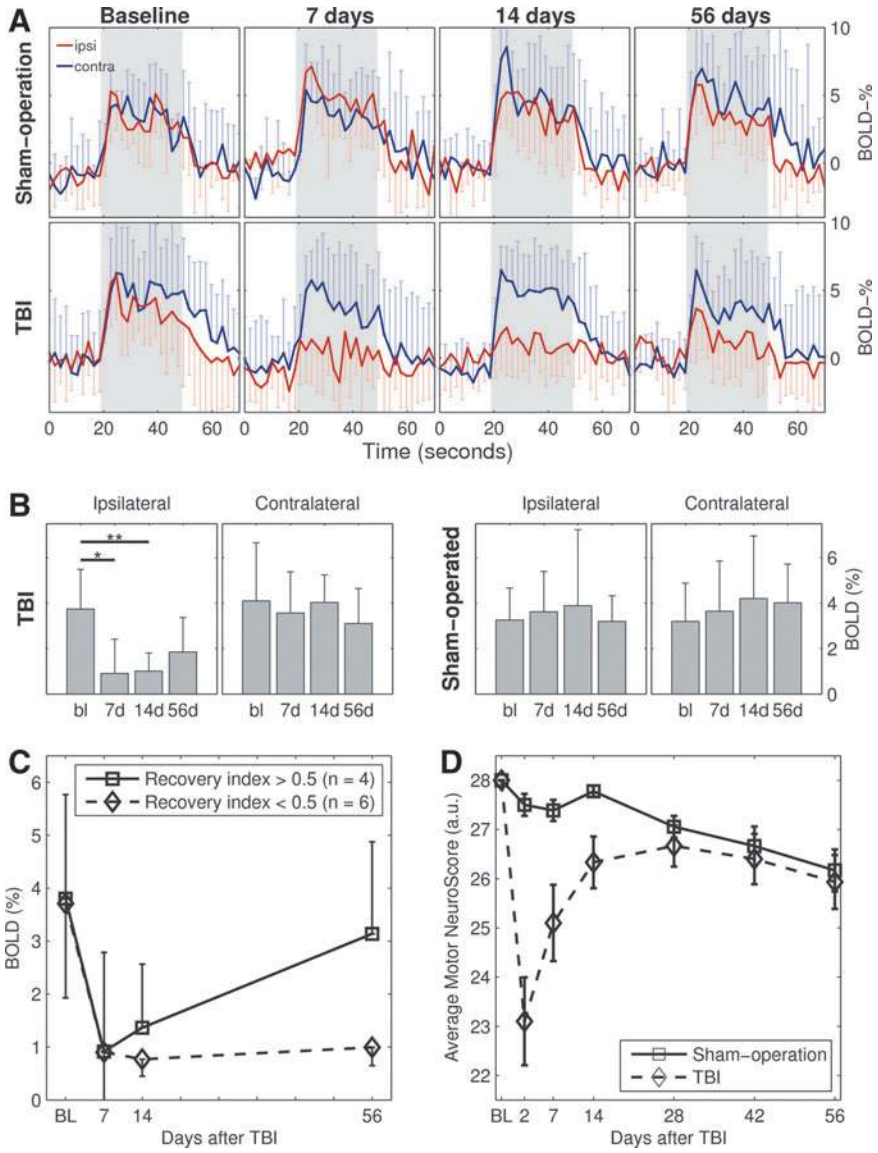

FIG. 4. Average functional MRI (fMRI) time series (group A) of one electrical forepaw stimulation block taken from a 2×2 voxel region of interest (ROI) in the primary somatosensory cortex ipsilateral (red line) or contralateral (blue line) to sham operation (upper panels) or lateral fluid-percussion induced brain injury (FPI) (lower panels). **(B)** The corresponding group averages of the estimated somatosensory blood-oxygen-level-dependent (BOLD) responses relative to the baseline. Injured rats had a reduction in the ipsilateral BOLD response when the values obtained at 7 days ($*p \leq 0.002$) or 14 days ($**p \leq 0.002$) post-traumatic brain injury (TBI) were compared with those at baseline. **(C)** The averaged BOLD responses of animals in group A that recovered (recovery index >0.5, solid line) and animals that did not recover (recovery index <0.5, dashed line) during the follow-up. **(D)** Recovery of motor function was assessed by behavioral neuroscore tests. Note that the score decreased by only ~ 5 points from the baseline, suggesting moderate rather than severe injury. Comparison of panels **B, C** and **D** shows that the somatosensory recovery occurs, but at a slow rate, and still remains below baseline at 56 days post-injury, whereas the rats showed almost complete motor recovery within ~ 3 weeks post-TBI. Color image is available online at www.liebertpub.com/neu

Contralaterally, the somatosensory BOLD responses and fMRI activation patterns did not show any significant changes in injured or sham operated rats. The fMRI activation patterns from representative injured and sham animals in group A are shown in Figure 3.

In line with data obtained in group A, no ipsilateral S1 activation was detected in any of the three rats available for analysis in group B at 2 days post-TBI.

To investigate whether a change in the CBF could contribute to S1 BOLD response in injured animals, we analyzed CBF in group B using ASL MRI. The mean CBF in the ipsilateral and contralateral S1 of injured rats did not differ at 2 days (78.7 ± 6.5 vs. 90.3 ± 17.3 mL/100 g/min) or at 35 days (67.0 ± 5.2 vs. 73.0 ± 11.4) post-TBI ($p > 0.5$). Correspondingly, CBF in the ipsilateral and contralateral S1 of the sham operated animals was (83.3 ± 2.2 vs. 76.4 ± 7.6 mL/100 g/min). These results indicate that our BOLD fMRI results were not biased by changes in the basal CBF.

Correlation of BOLD response in S1 with lesion volume and motor recovery. The ratio of ipsilateral and contralateral cortical volumes (R_{Cx}) or lesion volume did not correlate with BOLD response in the more rostrally located S1 at any time point.

In injured rats, the patterns of somatosensory and motor recovery during the 56 day follow-up were similar (Fig. 4B, D), even though the increase in S1 BOLD response occurred more slowly than the increase in neuroscore. We did not find any correlation between the recovery slopes for the S1 BOLD response and the neuroscore, suggesting that there was no association between the rate of somatosensory recovery and motor recovery in individual animals.

Behavioral impairment

The motor impairment of the injured rats was most severe at 2 days post-TBI, when composite neuroscore decreased to 23 (maximum 28), which also corresponds to moderate injury as previously reported.[32] (Fig. 4D). Thereafter, animals recovered during the first 2 weeks post-injury, and their composite neuroscores, were indistinguishable from those of sham operated animals at 28 days post-TBI (Fig. 4D). The recovery (defined as a slope of the recovery curve) was most rapid during the first 2–14 days post-TBI. None of the individual behavioral tests used to calculate the composite neuroscore correlated with the magnitude of the BOLD response.

Electrophysiology

As another measure of somatosensory recovery, we measured LFP responses in S1 in injured rats in group B. At 2 days post-TBI, the LFP response amplitudes in the ipsilateral S1 were on average only 24% of those contralaterally (Fig. 5A and B). At 35 days post-TBI, the ipsilateral LFP response amplitudes were on average 49% of those contralaterally (Fig. 5C and D). Sham operated rats had similar LFP responses bilaterally.

Histology

To understand the cellular basis of decreased BOLD response in the S1 of rats with TBI, in particular as the T_2-weighted MRI did not reveal any post-TBI structural damage in this region, we next assessed the neuronal damage along the somatosensory pathway at the end of the 56 day follow-up. Thionin-stained preparations indicated remarkable damage in the ventral posterior complex of the thalamus, which is the main relay region for somatosensory inputs directed to S1 (Fig. 6). In particular, the ventral posterolateral (VPL) and the ventral posteromedial (VPM) nuclei of the ventral posterior complex showed remarkable neurodegeneration, gliosis, and also calcifications (Fig. 6A), which are consistent with our previous study.[33] To semiquantitatively analyze the severity of damage, we divided the VPL into VPL1 and VPL2 and the VPM into VPM1, and VPM2 as shown in Figure 6E. The mean damage scores in each subregion were VPL1 2.0 ± 0.8, VPL2 2.4 ± 0.7, VPM1 1.4 ± 0.5, and VPM2 1.5 ± 0.7. Notably, the VPL2 that projects to the forepaw region of S1 showed severe damage.[34] Unexpectedly, the severity of damage in VPL2 did not correlate with decreased BOLD response in S1 at 56 days post-TBI ($r = -0.22$, $p > 0.5$) (Fig. 6F).

Next, we assessed whether the decrease in BOLD response would be associated with the severity of cortical neurodegeneration. As expected, we found remarkable neurodegeneration at the cortical injury site (Fig. 6B). However, the more rostrally located S1 appeared undamaged, including the S1 area that corresponded to the fMRI slice used for BOLD analysis (−1 mm from bregma).

As analysis of neurodegeneration did not provide a clear explanation for the differences in S1 BOLD response, we next investigated whether the decrease in BOLD response was associated with transection of fiber pathways. Analysis of myelin preparations revealed a remarkable reduction in the density of myelinated fibers in layer VI of the ipsilateral cortex. Importantly, the region of low

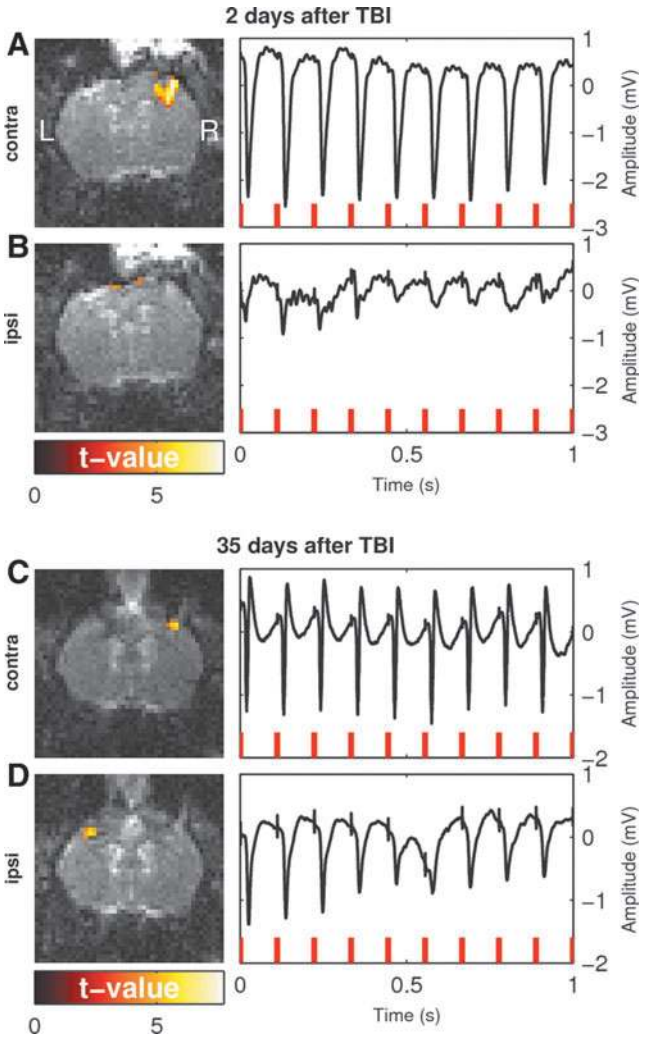

FIG. 5. Functional MRI (fMRI) activation maps overlaid with echo planar imaging (EPI) images and simultaneously measured local field potential responses from contralateral (panels **A** and **C**) and ipsilateral (panels **B** and **D**) somatosensory cortices in response to electrical forepaw stimulation. Data are shown from two representative animals from group **B**, from which one was imaged at 2 days (**A, B**) and the other at 35 days (**C, D**) after traumatic brain injury (TBI). The red lines denote stimulation events. Color image is available online at www.liebertpub.com/neu

fiber density extended from the primary impact area rostrally to layer VI of S1 ($p < 0.01$ as compared with the contralateral S1; Figs. 6A–E and 7A). Moreover, the reduction in the density of myelinated fibers in S1 correlated with the reduction in S1 BOLD response at 56 days post-TBI ($r = 0.71$, $p < 0.01$). Correlation was found when the ipsilateral S1 in both sham and TBI animals was included in the analysis (Fig. 7E) as well as when the correlation analysis was performed including the TBI animals only ($r = 0.66$, $p < 0.05$). A higher density of remaining myelin fibers was also correlated with a faster BOLD recovery rate ($r = 0.74$, $p < 0.02$). The myelin density in layer VI of the ipsilateral S1 showed on average a 20% reduction as compared with the contralateral S1 of the same animals ($p < 0.002$). Further analysis indicated that in animals with a persistently reduced BOLD response, the myelin density was 18% lower than that of rats with BOLD recovery ($p < 0.05$), and 28% lower than that of sham operated animals ($p < 0.03$).

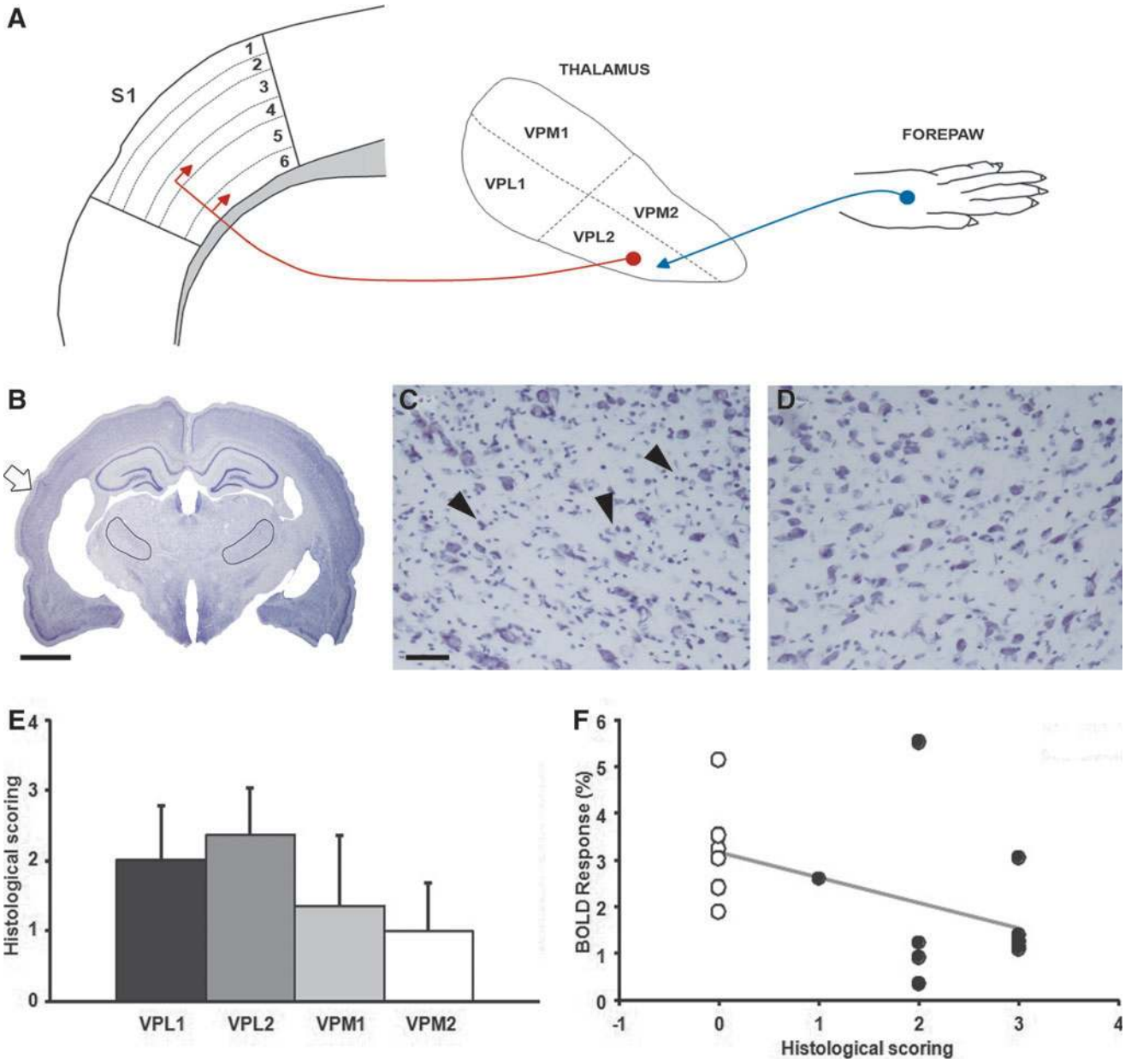

FIG. 6. **(A)**Schematic representation of the pathway that conveys the electrical stimulation from the forepaw to the somatosensory cortex (S1) via the ventroposterolateral nucleus of the thalamus (VPL). **(B)** Low-power photomicrograph of a thionin-stained section from a rat with traumatic brain injury (TBI) 84 days earlier. The impact site is indicated with an open arrow. The black outline indicates the location of the ventroposteromedial (VPM) and VPL thalamic nuclei. Scale bar equals 2 mm. **(C, D)** Higher-power photomicrographs of thionin-stained sections of the medial aspect of the VPL (VPL2) from the animal in panel **B**. Panel **C** is ipsilateral and panel **D** is contralateral to the TBI. Note reduced neuronal density and increased gliosis (black arrowheads) ipsilaterally in panel **C**. The scale bar equals 50 μm. **(E)** Bar graphs summarizing the severity of neurodegeneration and associated gliosis in different parts of the VPL (VPL1 and VPL2) and VPM (VPM1 and VPM2) in thionin-stained preparations at 84 days post-TBI (see text for scoring). The damage was most prominent in VPL2 that relays the somatosensory information from the thalamus to S1. **(F)** We did not find any correlation between the severity of histological damage in the ipsilateral VPL2 and blood-oxygen-level-dependent (BOLD) response (%) in the ipsilateral S1 ($r = -0.22$, $p > 0.5$). Symbols: white dots, ipsilateral VPL2 damage score in sham operated rats; black dots, corresponding data from rats with TBI. Color image is available online at www.liebertpub.com/neu

Discussion

The present study was designed to test a hypothesis that BOLD fMRI can be used to monitor functional recovery in the S1 cortex after experimental TBI. To address the challenge, we induced TBI by using lateral FPI in adult rats, and monitored the severity of damage and functional recovery by using structural and functional MRI, electrophysiology, behavioral testing, and histology. All of the rats had a reduced BOLD response during the 1st week post-TBI in the ipsilateral S1, which is located rostromedially to the primary lesion site, and showed no changes in anatomical T_2-weighted MRI. Forty percent of these animals showed recovery of

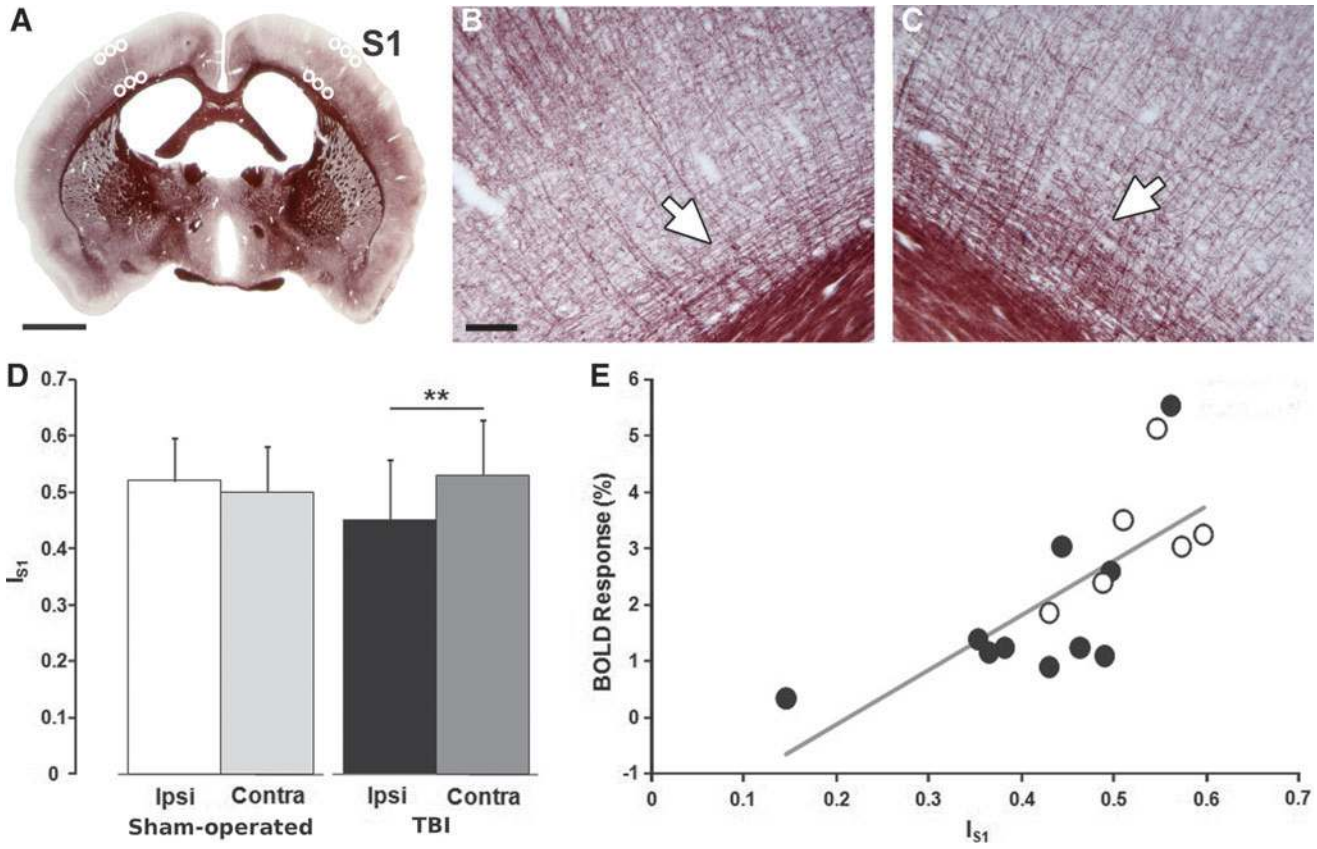

FIG. 7. **(A)** A low-power photomicrograph of a myelin-stained section of a rat that had experienced traumatic brain injury (TBI) 84 days earlier. The white circles indicate the regions of interest (ROIs) that were used for quantification of the density of myelinated fibers in layer VI of the S1. The scale bar equals 2 mm. **(B, C)** Higher-power photomicrographs of myelin-stained fibers from the section in panel **A**. Panel **B** is from the ipsilateral, and panel **C** is from the contralateral side. Note the reduction in the density of myelinated fibers ipsilaterally in panel **B** (white arrows). The scale bar equals 100 μm. **(D)** Bar graphs summarizing the density of myelinated fibers in layer VI of the S1 (I_{S1}) in sham operated and injured (TBI) rats both ipsilaterally and contralaterally. At 84 days post-TBI, the fiber density was reduced in injured animals ipsilaterally ($^{**}p < 0.01$). **(E)** The lower the density of myelinated fibers in layer VI, the more reduced the blood-oxygen-level-dependent (BOLD) response (%) in the ipsilateral S1 (at 56 days post-TBI) ($r = 0.71$, $p < 0.01$). Symbols; the white dots indicate sham operated rats; black dots indicate rats with TBI. Color image is available online at www.liebertpub.com/neu

the BOLD response during the 56 day follow-up. Unexpectedly, no association was found between the recovery in BOLD response and the volume of the cortical lesion. Instead, the functional recovery was found in rats with preserved myelinated fibers in layer VI of S1. To our knowledge, this is the first study demonstrating that functional recovery can be monitored using fMRI in experimental TBI. It also shows that a lack of functional recovery that is distant to the primary injury site may relate to axonal injury rather than neurodegeneration, which may remain undetectable in structural MRI.

The functionally compromised area extends beyond the primary lesioned cortex in TBI

Based on our previous experience, we adjusted the FPI to $\sim$2.0 atm to produce moderate TBI.[32] The negligible mortality and small decline in neuroscore from 28 to 23 by the 2nd post-injury day both support the conclusion that animals included in the present follow-up had experienced moderate TBI. Also, the volumes of the cortical lesion in group B at 2 days post-injury were comparable to those in animals with moderate injury imaged at 3 days post-TBI reported previously (data not shown).[32]

As in our previous experiments, lateral FPI triggered a cortical lesion that was located $\sim$3–6 mm caudal to S1. Even though S1 appeared structurally normal based on T_2-weighted MRI and analysis of thionin-stained histological preparations, the fMRI activation in S1 was lost either completely or partially in 80% of injured animals, and the strength of the BOLD response was reduced in all injured animals during the 1st post-injury week. These data show that functional impairment after moderate lateral FPI extends beyond the area of primary cortical injury. As the loss of neurons in S1 was minimal, it became fascinating to see whether the remaining somatosensory network could repair its function, and whether we could monitor the recovery process by using fMRI.

fMRI detects functional recovery in a subgroup of animals after TBI

The follow-up of animals for $\sim$2 months post-TBI demonstrated recovery of somatosensory function in 40% of the rats as assessed by using the S1 BOLD response as well as measurement of LFPs. The improvement was, however, slower than that of motor function assessed by neuroscore. On average, the relative reduction in the S1 BOLD responses as compared with pre-TBI BOLD responses was 76% at 7 days, 73% at 14 days, and only 51% at 56 days post-TBI. Analysis of data from individual animals indicated that in 4 of 10 rats the recovery of the BOLD response was almost

complete by 56 days post-TBI, that is, it was decreased by < 1 SD of the baseline mean. Although understanding the exact mechanism of the recovery is beyond the scope of this study, it is well documented that post-injury synaptic plasticity associates with functional recovery after TBI.[35,36] Our success in monitoring the recovery process noninvasively in a well-characterized animal model of TBI creates a scenario in which fMRI could be a useful tool to monitor the efficacy of novel recovery-enhancing treatments for TBI in proof-of-principle and pre-clinical trials.

The functional defect was associated with decreased density of myelinated axons in S1 rather than thalamic damage

We were, however, puzzled by the finding that somatosensory recovery occurred only in a subgroup of injured animals even though they all lacked neurodegeneration in S1, and they all had a normal S1 on T_2-weighted MRI. Therefore, we next assessed whether the histologically detectable lesion at other levels of the thalamocortical somatosensory pathway could explain the persistent impairment in some animals.

We found substantial neuronal loss, gliosis, and even calcifications in the ipsilateral thalamus. In particular, the damage was prominent in the VPL nucleus that relays sensory information to the forepaw region of S1.[34] Unexpectedly, there was no correlation between the severity of neurodegeneration in the VPL nucleus (or other parts of the ventral posterior nucleus) and the S1 BOLD response. It is important to note that not all neurons had died in the VPL nucleus, suggesting that the remaining cells were sufficient to relay the somatosensory signal to S1, and trigger the BOLD response.

As the thalamic neurodegeneration did not explain the loss of BOLD response in a subgroup of animals, we next assessed whether the shearing injury of myelinated fibers at the interface between the cortical gray and white matter could contribute to the persistent functional impairment in S1.[37] Microscopic analysis of myelin preparations revealed reduced density of myelinated fibers in layer VI of the ipsilateral cortex, which extended beyond the primary cortical lesion rostromedially up to S1. Moreover, we found a strong correlation between the density of myelinated fibers and the BOLD recovery rate as well as between the fiber density and BOLD response at 56 days post-TBI.

Taken together, somatosensory recovery can be verified by using BOLD fMRI, but only in animals with well-preserved myelinated fibers in layer VI of S1. This is feasible, as it has been shown that afferent inputs from the VPL nucleus directed to S1 pass through layer VI to innervate the upper layers, to evoke the BOLD response in S1. Consequently, the lack of recovery of the S1 BOLD response suggests a shearing injury in an apparently otherwise normal cortex.

Methodological considerations

We next assessed whether hemodynamic disturbance in the damaged cortex could have contributed to the reduced BOLD fMRI response. In particular, we were interested whether reduced BOLD signal in the ipsilateral S1 could be explained by uncoupling of the hemodynamic and neuronal responses. This possibility was explored using simultaneous fMRI/LFP measurements at 2 and 35 days post-TBI. Our data show that reduced BOLD response in the ipsilateral S1 is associated with reduced LFP response, indicating that the coupling between hemodynamic and neuronal responses is preserved.

Post-TBI perfusion changes could also potentially contribute to the BOLD responses in the ipsilateral S1, as cerebrovascular and hemodynamic changes are known to be involved in secondary damage after TBI. We measured CBF using ASL MRI and found no significant changes in perfusion outside the primary lesion area. In a recent study, widespread ipsilateral and contralateral hypoperfusion were reported in the rat cortex and hippocampus bilaterally, as well as in the thalamus ipsilaterally after severe lateral FPI.[8] In addition, in the study by Liu and colleagues,[10] widespread hypometabolism was found in rats with FPI in the ipsilateral cortex, hippocampus, and amygdalae. However, severe FPI models (3.2–3.5 atm fluid pressure) were used in these studies, and it therefore appears that the delayed hypoperfusion response is dependent upon the severity of the initial impact, and did not contribute to the results of the present study.

Hypercarbia is a common consequence of extended anesthesia without ventilation. We found moderately elevated pCO_2 levels in our spontaneously breathing animals. CO_2 is a well- known vasodilator and it increases both the basal CBF and CBV, and, consequently, this reduces the amplitude of the BOLD response. However, we were able to detect robust BOLD responses in the order of 3–5% using spin-echo echo planar imaging (EPI) at 4.7 T. This is a typical BOLD response magnitude in rats during forepaw stimulation, and it suggests that the influence of pCO_2 on our fMRI measurements must have been relatively small. Furthermore, there was no difference in blood gas measurements between sham operated and TBI animals, which rules out any blood gas variability as a major explanatory factor for fMRI changes induced by TBI.

Conclusions

Our study provides the first evidence that functional recovery after experimental TBI induced by lateral FPI of moderate severity can be monitored by using fMRI. Importantly, fMRI can also pinpoint pathologies that are not readily evident in structural MRI. As fMRI is already used in human studies, the present findings encourage exploration of the usefulness of fMRI as a noninvasive prognostic translational biomarker for post-TBI outcomes and therapy responses.

Acknowledgments

This work was supported by Academy of Finland (grant numbers 123579, 252511, 132970), the Juselius Foundation, Orion-Farmos Research Foundation, and the strategic funding of the University of Eastern Finland (UEF-Brain). We thank Jarmo Hartikainen and Maarit Pulkkinen for technical assistance, and Dr. Nick Hayward of Scientific English, UK, for revising the language of this manuscript.

Author Disclosure Statement

No competing financial interests exist.

References

1. Hyder, A. A., Wunderlich, C. A., Puvanachandra, P., Gururaj, G., and Kobusingye, O. C. (2007). The impact of traumatic brain injuries: a global perspective. NeuroRehabilitation 22, 341–353.
2. Loane, D. J., and Faden, A. I. (2010). Neuroprotection for traumatic brain injury: translational challenges and emerging therapeutic strategies. Trends Pharmacol. Sci. 31, 596–604.
3. McAllister, T. W. (2011). Neurobiological consequences of traumatic brain injury. Dialogues Clin. Neurosci. 13, 287–300.
4. Pitkanen, A., and Lukasiuk, K. (2011). Mechanisms of epileptogenesis and potential treatment targets. Lancet Neurol. 10, 173–186.

5. Pitkanen, A., and McIntosh, T. K. (2006). Animal models of post-traumatic epilepsy. J Neurotrauma 23, 241–261.
6. Chaiwat, O., Sharma, D., Udomphorn, Y., Armstead, W. M., and Vavilala, M. S. (2009). Cerebral hemodynamic predictors of poor 6-month Glasgow Outcome Score in severe pediatric traumatic brain injury. J Neurotrauma 26, 657–663.
7. Hattori, N., Huang, S. C., Wu, H. M., Liao, W., Glenn, T. C., Vespa, P. M., Phelps, M. E., Hovda, D. A., and Bergsneider, M. (2003). PET investigation of post-traumatic cerebral blood volume and blood flow. Acta Neurochir. Suppl. 86, 49–52.
8. Hayward, N. M., Tuunanen, P. I., Immonen, R., Ndode–Ekane, X. E., Pitkanen, A., and Grohn, O. (2011). Magnetic resonance imaging of regional hemodynamic and cerebrovascular recovery after lateral fluid-percussion brain injury in rats. J. Cereb. Blood Flow Metab. 31, 166–177.
9. Kim, J., Whyte, J., Patel, S., Avants, B., Europa, E., Wang, J., Slattery, J., Gee, J. C., Coslett, H. B., and Detre, J. A. (2010). Resting cerebral blood flow alterations in chronic traumatic brain injury: an arterial spin labeling perfusion FMRI study. J Neurotrauma 27, 1399–1411.
10. Liu, Y. R., Cardamone, L., Hogan, R. E., Gregoire, M. C., Williams, J. P., Hicks, R. J., Binns, D., Koe, A., Jones, N. C., Myers, D. E., O'Brien, T. J., and Bouilleret, V. (2010). Progressive metabolic and structural cerebral perturbations after traumatic brain injury: an in vivo imaging study in the rat. J. Nucl. Med. 51, 1788–1795.
11. Frey, L. C. (2003). Epidemiology of posttraumatic epilepsy: a critical review. Epilepsia 44, Suppl. 10, 11–17.
12. Pitkanen, A., Immonen, R. J., Grohn, O. H., and Kharatishvili, I. (2009). From traumatic brain injury to posttraumatic epilepsy: what animal models tell us about the process and treatment options. Epilepsia 50, Suppl. 2**,** 21–29.
13. Cullen, D. K., Vernekar, V. N., and LaPlaca, M. C. (2011). Trauma-induced plasmalemma disruptions in three-dimensional neural cultures are dependent on strain modality and rate. J Neurotrauma 28, 2219–2233.
14. Ding, M. C., Wang, Q., Lo, E. H., and Stanley, G. B. (2011). Cortical excitation and inhibition following focal traumatic brain injury. J. Neurosci. 31, 14,085–14,094.
15. Kawai, N., Maeda, Y., Kudomi, N., Yamamoto, Y., Nishiyama, Y., and Tamiya, T. (2010). Focal neuronal damage in patients with neuropsychological impairment after diffuse traumatic brain injury: evaluation using (1)(1)C-flumazenil positron emission tomography with statistical image analysis. J. Neurotrauma 27, 2131–2138.
16. Garnett, M. R., Blamire, A. M., Corkill, R. G., Rajagopalan, B., Young, J. D., Cadoux–Hudson, T. A., and Styles, P. (2001). Abnormal cerebral blood volume in regions of contused and normal appearing brain following traumatic brain injury using perfusion magnetic resonance imaging. J. Neurotrauma 18, 585–593.
17. Laatsch, L., and Krisky, C. (2006). Changes in fMRI activation following rehabilitation of reading and visual processing deficits in subjects with traumatic brain injury. Brain Inj. 20, 1367–1375.
18. Mayer, A. R., Mannell, M. V., Ling, J., Elgie, R., Gasparovic, C., Phillips, J. P., Doezema, D., and Yeo, R. A. (2009). Auditory orienting and inhibition of return in mild traumatic brain injury: a FMRI study. Hum. Brain Mapp. 30, 4152–4166.
19. Mayer, A. R., Mannell, M. V., Ling, J., Gasparovic, C., and Yeo, R. A. (2011). Functional connectivity in mild traumatic brain injury. Hum. Brain Mapp. 32, 1825–1835.
20. Morales, D., McIntosh, T., Conte, V., Fujimoto, S., Graham, D., Grady, M. S., and Stein, S. C. (2006). Impaired fibrinolysis and traumatic brain injury in mice. J. Neurotrauma 23, 976–984.
21. Hayward, N. M., Immonen, R., Tuunanen, P. I., Ndode–Ekane, X. E., Grohn, O., and Pitkanen, A. (2010). Association of chronic vascular changes with functional outcome after traumatic brain injury in rats. J. Neurotrauma 27, 2203–2219.
22. Immonen, R., Heikkinen, T., Tahtivaara, L., Nurmi, A., Stenius, T. K., Puolivali, J., Tuinstra, T., Phinney, A. L., Van Vliet, B., Yrjanheikki, J., and Grohn, O. (2010). Cerebral blood volume alterations in the perilesional areas in the rat brain after traumatic brain injury—comparison with behavioral outcome. J. Cereb. Blood Flow Metab. 30, 1318–1328.
23. Henninger, N., Sicard, K. M., Li, Z., Kulkarni, P., Dutzmann, S., Urbanek, C., Schwab, S., and Fisher, M. (2007). Differential recovery of behavioral status and brain function assessed with functional magnetic resonance imaging after mild traumatic brain injury in the rat. Crit. Care Med. 35, 2607–2614.
24. Kharatishvili, I., Nissinen, J. P., McIntosh, T. K., and Pitkanen, A. (2006). A model of posttraumatic epilepsy induced by lateral fluid-percussion brain injury in rats. Neuroscience 140, 685–697.
25. McIntosh, T. K., Vink, R., Noble, L., Yamakami, I., Fernyak, S., Soares, H., and Faden, A. L. (1989). Traumatic brain injury in the rat: characterization of a lateral fluid-percussion model. Neuroscience 28, 233–244.
26. Paxinos, G., and Watson, C. (1998). *The Rat Brain in Stereotaxic Coordinates,* 4th ed. Academic Press: San Diego.
27. Gruetter, R. (1993). Automatic, localized in vivo adjustment of all first- and second-order shim coils. Magn. Reson. Med. 29, 804–811.
28. Williams, D. S., Detre, J. A., Leigh, J. S., and Koretsky, A. P. (1992). Magnetic resonance imaging of perfusion using spin inversion of arterial water. Proc. Natl. Acad. Sci. U. S. A. 89, 212–216.
29. Thompson, H. J., Lifshitz, J., Marklund, N., Grady, M. S., Graham, D. I., Hovda, D. A., and McIntosh, T. K. (2005). Lateral fluid percussion brain injury: a 15-year review and evaluation. J. Neurotrauma 22, 42–75.
30. Pitkanen, A., Tuunanen, J., and Halonen, T. (1996). Vigabatrin and carbamazepine have different efficacies in the prevention of status epilepticus induced neuronal damage in the hippocampus and amygdala. Epilepsy Res. 24, 29–45.
31. Silva, A. C., Koretsky, A. P., and Duyn, J. H. (2007). Functional MRI impulse response for BOLD and CBV contrast in rat somatosensory cortex. Magn. Reson. Med. 57, 1110–1118.
32. Kharatishvili, I., Sierra, A., Immonen, R. J., Grohn, O. H., and Pitkanen, A. (2009). Quantitative T2 mapping as a potential marker for the initial assessment of the severity of damage after traumatic brain injury in rat. Exp. Neurol. 217, 154–164.
33. Lehto, L. J., Sierra, A., Corum, C. A., Zhang, J., Idiyatullin, D., Pitkanen, A., Garwood, M., and Grohn, O. (2012). Detection of calcifications in vivo and ex vivo after brain injury in rat using SWIFT. Neuroimage 61, 761–772.
34. Liao, C. C., and Yen, C. T. (2008). Functional connectivity of the secondary somatosensory cortex of the rat. Anat. Rec. (Hoboken) 291, 960–973.
35. Dijkhuizen, R. M., Singhal, A. B., Mandeville, J. B., Wu, O., Halpern, E. F., Finklestein, S. P., Rosen, B. R., and Lo, E. H. (2003). Correlation between brain reorganization, ischemic damage, and neurologic status after transient focal cerebral ischemia in rats: a functional magnetic resonance imaging study. J. Neurosci. 23, 510–517.
36. Goldstein, L. B. (2003). Neuropharmacology of TBI-induced plasticity. Brain Inj. 17, 685–694.
37. Graham, D. I., Raghupathi, R., Saatman, K. E., Meaney, D., and McIntosh, T. K. (2000). Tissue tears in the white matter after lateral fluid percussion brain injury in the rat: relevance to human brain injury. Acta Neuropathol. 99, 117–124.

Address correspondence to:
Olli H. Gröhn, PhD
Department of Neurobiology
A. I. Virtanen Institute for Molecular Sciences
University of Eastern Finland
P.O. Box 1627
FI-70211 Kuopio
Finland

E-mail: olli.grohn@uef.fi